Effective multidimensional crossover behavior in a one-dimensional voter model with long-range probabilistic interactions

D. E. Rodriguez,[1,*] M. A. Bab,[1,2] and E. V. Albano[2,3]

[1]*Instituto de Investigaciones Fisicoquímicas Teóricas y Aplicadas (INIFTA), Facultad de Ciencias Exactas, Universidad Nacional de La Plata, CCT-La Plata CONICET, Suc. 4, CC 16, 1900 La Plata, Argentina*

[2]*Departamento de Física, Facultad de Ciencias Exactas, Universidad Nacional de La Plata, La Plata, Argentina*

[3]*Instituto de Física de Liquidos y Sistemas Biologicos (IFLYSIB), Calle 59 N 789, 1900 La Plata, Argentina*

(Received 4 June 2010; revised manuscript received 31 October 2010; published 13 January 2011)

A variant of the standard voter model, where a randomly selected site of a one-dimensional lattice ($d = 1$) adopts the state of another site placed at a distance r from the previous one, is proposed and studied by means of numerical simulations that are rationalized with the aid of dynamical and finite-size scaling arguments. The distance between the two sites is also selected randomly with a probability given by $P(r) \propto r^{-(d+\sigma)}$, where σ is a control parameter. In this way one can study how the introduction of these long-range interactions influences the dynamic behavior of the standard voter model with nearest-neighbor interactions. It is found that the dynamics strongly depends on the range of the interactions, which is parameterized by σ, leading to an interesting effective multidimensional crossover behavior, as follows. (a) For $\sigma < 1$ ordering is no longer observed and the average interface density [$\rho(t)$] assumes a steady state in the thermodynamic limit. Instead, for finite-size systems an exponential decay with a characteristic time (τ) that increases with the size is observed. This behavior resembles the scenario corresponding to the short-range voter model for $d > 2$, as well as the case of both scale-free and small-world networks. (b) For $\sigma > 1$, an ordering dynamics is observed, such that $\rho(t) \propto t^{-\alpha}$, where the exponent α increases with σ until it reaches the value $\alpha = 1/2$ for $\sigma \geqslant 5$, which corresponds to the behavior of the standard voter model with short-range interactions in $d = 1$. (c) Finally, for $\sigma \approx 1$ we show evidence of a critical-type behavior as in the case of the critical dimension ($d_c = 2$) of the standard voter model.

DOI: 10.1103/PhysRevE.83.011110 PACS number(s): 64.60.Ht, 05.50.+q, 05.70.Ln

I. INTRODUCTION

The standard voter model (SVM) is one of the simplest models with short-range interactions that addresses the competition of two equivalent but excluding options. In the SVM each site of a lattice is characterized by a variable s_i, which can assume only two values ($s_i = \pm 1$) that fully specify the state of site i. Then an elementary dynamic step consists of selecting one site at random and assigning to it the state of one of its nearest neighbors, also randomly chosen. The SVM has the particularity of being one of a very few models exactly solvable in regular lattices for any arbitrary dimension [1,2], and recently has also been solved in uncorrelated networks by using a mean-field approach [3]. Its ordering dynamics shows the interesting behavior [1,4] that for $d \leqslant 2$ the SVM converges irreversibly to one of two possible ordered states where all sites take the same option; that is, the system has two equivalent absorbing states. In contrast, above the critical dimension ($d > d_c = 2$) as well as in some complex networks, such as small-world [5] and scale-free networks [6,7], it is known that the system does not reach any ordered state in the thermodynamic limit but, instead, a stationary active state with coexisting domains always prevails.

By considering the state s_i of the ith site as a spin variable, the SVM mimics the evolution of a magnetic (Ising-like) system at zero temperature ($T = 0$) and in the absence of surface tension [4,8]. Recently, a comparison between the dynamics of the SVM and that of the Ising model with Glauber dynamics at $T = 0$, in complex networks, has been reported [7]. Furthermore, due to the self-ordering nature of its dynamic evolution, the SVM can also be used to characterize different network configurations.

In contrast, the SVM can also be conceived as a simple social model for opinion formation. In fact, by assuming that the sites of the sample are occupied by agents having only two possible states of opinion, representing, for example, two candidates in a ballotage election and buying-selling a product, either the dynamics may evolve into two equivalent absorbing states with the agents having the same opinion or, eventually, the consensus may no longer be achieved. Of course, the nature of the final state depends on the dimensionality and the structure of the underlying network. However, this social approach is better suited for high-dimensional regular lattices or scale-free networks where one has a dramatic increase in the number of neighbors when large distances are considered.

Another application of the SVM arises in the field of heterogeneous catalyzed reactions where it can be mapped into a dimer-dimer reaction model [9]. Further interest in the SVM is due to the fact that it defines a broad type of universality class [8]. In fact, order-disorder transitions in Z_2-symmetric absorbing states models that are driven by interfacial noise generally belong to the so-called voter universality class.

Apart from the SVM itself, several variants have been proposed aimed, on the one hand, to test the robustness of its universality class [8] and, on the other hand, to attempt the description of more complex situations beyond the usual interest in the field of condensed matter and statistical physics [11]. Among these variants, one could mention the nonlinear voter model [12], the vacillating voter model [13], the q-voter model [14], etc.

*rodrigdiego@gmail.com

Within this context, the aim of this work is to propose and study a one-dimensional voter model with probabilistic long-range interactions weighted with the distance r as $P(r) \propto r^{-(d+\sigma)}$, where d is the dimension and σ is a parameter that controls the length of the interaction. The proposed link-update model provides a useful and simple scenario for understanding the effect of the control parameter σ on the dynamic behavior, which seems to play a role analogous to a dimensional variation.

The manuscript is organized as follows: in Sec. II we give a brief theoretical background description of the voter model with long-range interactions and details of the simulation method. Section III is devoted to presenting and discussing our results on the dynamic behavior of the long-range voter model, and finally, our conclusions are stated in Sec. IV.

II. SIMULATION METHOD

A. Definitions and theoretical background

The order parameter often used for the SVM is the average interface density ρ, where one interface site is defined by two next-neighbor sites in different states. In this way, by starting the system from fully disordered configurations, the average interface density decreases as domains with the same magnetization or state of opinion grow. Also, $\rho = 0$ indicates that one of the absorbing states (consensus) has been reached. The asymptotic dynamic behavior of $\rho(t)$ in regular networks is described as follows [1,9]: (i) for $d < 2$ a coarsening process causes the decay of the order parameter according to a power law given by $\rho(t) \propto t^{-\alpha}$, with $\alpha = (1 - D/2)$; (ii) at the critical dimension ($d_c = 2$) there is a slower ordering with a logarithm dependence such as $\rho(t) \propto (\ln(t))^{-1}$; and (iii) for $d > 2$ the order parameter evolves toward a constant value ρ_0, thus the interface density presents an initial decaying transient indicating the onset of ordering, but then it reaches a partially ordered state where the coarsening process stops.

For finite-size systems the lifetime of the interfaces is always finite in any regime, even for $d > 2$; that is, after some time period the system departs from the expected behavior in the thermodynamic limit and always evolves into one of the two available absorbing states. This lifetime and its scaling behavior for different sizes are useful to characterize the dynamic regimes. However, it is important to distinguish that the lifetime (τ) for each regime depends on different processes acting on the dynamic evolution: for the $d > 2$ regime τ is determined by the likelihood of a fluctuation capable of driving the system into one of the two absorbing states, while when coarsening processes are at work, τ is determined by the presence of the boundaries.

Furthermore, the scaling dependence of τ on the size of the system can also be used to classify different types of networks. In fact, in regular networks one has that (i) for $d = 1$ the coarsening process departs from the power law and assumes a faster decay, giving $\tau(L) \propto L^2$ [6]; (ii) in $d_c = 2$ there is already a logarithmic dependence such as $\tau(L) \propto L \ln(L)$ [6]; and (iii) for $d > d_c$, the finite-size effect appears in the characteristic time of the exponential decay, where $\tau(L) \propto L$ is obtained [9].

In contrast, in complex networks with infinite effective dimension, such as small-world networks [5,15], the scale-free Barabási Albert network [7], random graphs [16], random networks, and scale-free networks [6], the ordering process is not completed. It is worth mentioning that for finite-size networks an exponential decay of the interface density is found and an effective steady sate can be estimated by the slower part of this decay, which only leads to a true steady sate in the thermodynamic limit.

In the case of fractal networks exhibiting discrete scale invariance, where an ordering process is present for fractal dimensions $d_f < 2$ [10,17,18], the power-law decay is modulated by logarithmic-periodic oscillations linking the topology of the substrate with the dynamics.

B. The voter model with long-range probabilistic interactions (LRVM)

Spin models with long-range interactions that decay with the distance have attracted much attention due to both their theoretical interest in condensed matter and statistical physics and their relationship with neural system modeling, where far-away neurons interact through an action potential that decays slowly along the axon. To study how the introduction of long-range interactions affects the ordering dynamics of the SVM, here we introduce a modified version where a given site can assume the state of any other site placed at a distance r, and selected with a probability that is given by a distribution P(r), which decays algebraically with r as $P(r) \propto r^{-(d+\sigma)}$, where σ is a parameter that controls the strength of the long-range interactions and d is the dimensionality. In this work the influence of the control parameter on the ordering dynamics is carefully characterized by means of extensive numerical simulations performed for different values of σ.

The LRVM in a one-dimensional lattice of L sites with periodic boundary conditions is considered. The studied system sizes are varied from $L = 5 \times 10^2$ up to $L = 5 \times 10^5$.

To study the ordering dynamics, the simulations are started from random initial conditions where a variable $s_i = \pm 1$ is randomly associated with each site of the lattice. The dynamics is implemented by randomly choosing a site that subsequently adopts the state of another site selected in a randomly chosen direction and placed at a distance r that is determined from a distance probability distribution $P(r) \propto r^{-(d+\sigma)}$. Several long-range interactions can be modeled by sweeping the parameter σ that controls the breadth of the distribution. The used values of the control parameter are chosen in the interval ($0.1 \leqslant \sigma \leqslant 10$). The Monte Carlo time step (MCS) involves L trials, so that each site is updated once on average during 1 MCS.

The order parameter $[\rho(t)]$ is calculated by means of the following definition:

$$\rho = \left\langle \frac{\sum_{i=1}^{L-1}(1 - s_i s_{i+1})/2}{2(L-1)} \right\rangle, \tag{1}$$

where the brackets indicate the average of the samples over a number n_s of different realizations, with $5 \times 10^2 \leqslant n_s \leqslant 4 \times 10^3$ depending on the lattice size and on the value of σ. In this way a fully disordered configuration corresponds to $\rho(t) = 0.5$, and the absorbing states to $\rho(t) = 0$. To determine

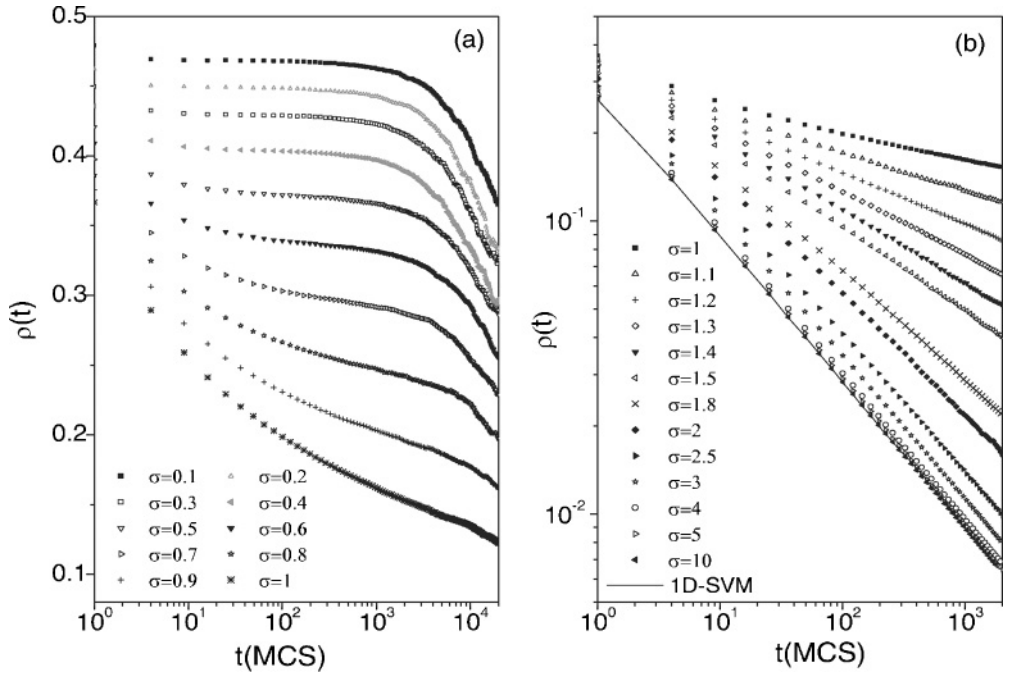

FIG. 1. (a) Linear-log plots of the time evolution of the average interface density (ρ) measured for values of the control parameter σ in the interval $0.1 \leqslant \sigma \leqslant 1$. (b) Log-log plots of the time evolution of the average interface density (ρ) measured for different values of the control parameter σ in the interval $1 \leqslant \sigma \leqslant 10$. The solid line corresponds to our results for the dynamic evolution of the 1D SVM. Results obtained using a system of size $L = 10^5$ and averaging over $n_s = 500$ realizations. More details in the text.

the values corresponding to the steady states of $\rho(t)$, averages are calculated by taking only realizations that have not decayed to $\rho(t) = 0$. We have also analyzed the scaling behavior of the lifetime of the partially ordered state with the system size, to compare the obtained results with already known results corresponding to the SVM and to other types of network configurations, such as small-world [5], scale-free Barabási-Albert [7], random, and random scale-free networks [6,7].

III. RESULTS AND DISCUSSION

The analysis of the simulation results is divided into two sections, as follows. (A) The first one corresponds to the study of the different types of dynamic behavior of the average interface density (ρ), observed for several values of σ in the interval $0.1 \leqslant \sigma \leqslant 10$. (B) The second one involves the study of the finite-size effects observed for the different ordering regimes characteristic of the system.

A. Analysis and discussion of the time evolution

Figure 1 shows the time dependence of the average interface density, as obtained for different values of the control parameter with $0.1 \leqslant \sigma \leqslant 10$. As shown in Fig. 1(a), for $0.1 \leqslant \sigma \leqslant 0.7$ the system exhibits an initial transient decrease in $\rho(t)$ that is indicative of a partial ordering. Subsequently, the system undergoes an exponential decay, although it is expected that in the thermodynamic limit these values of σ will lead to steady states with $[0 < \rho(t) < 1/2]$.

The value corresponding to the steady state of the averaged interface density (ρ_0) was estimated from the prefactor of a fitted exponential decay for different sizes [see Eq. (3)], as discussed in Sec. III B, resulting in a dependence of ρ_0 on the control parameter σ [see Fig. 2(a)].

For $1 < \sigma < 10$ [see Fig. 1(b)] the interface density shows a power-law decay of the form $\rho(t) \propto t^{-\alpha}$, where α is an exponent. This behavior can be related to the presence of a coarsening process. The exponent of the power law (α) increases with σ, as shown in Fig. 2(b), reaching the value corresponding to the one-dimensional (1D) SVM ($\alpha = 0.5$) for $\sigma = 5$; see also Fig. 1(b), where results obtained for the 1D SVM curve are shown as the solid line for the sake of comparison. Furthermore, a numeric derivative of the curve $\alpha(\sigma)$ [see the inset in Fig. 2(b)] shows a maximum for values

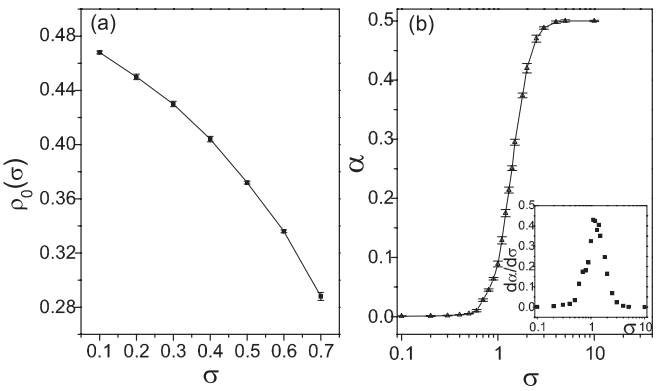

FIG. 2. Plots of the ρ_0 value of the steady-state interface density (a), and the power-law exponent α (b), as a function of the control parameter σ. (b) Inset: linear-log plot of the numerical derivative of $\alpha(\sigma)$ with respect to σ, which shows a peak close to $\sigma = 1.0(1)$. More details in the text.

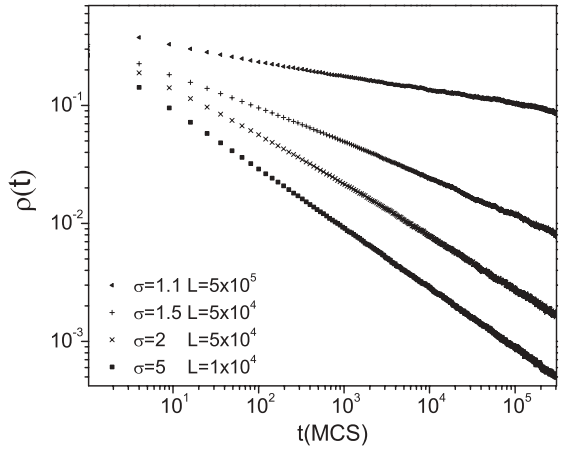

FIG. 3. Log-log plots of the time evolution of the average interface density ρ as obtained for different representative values of the control parameter σ in the coarsening regime. More details in the text.

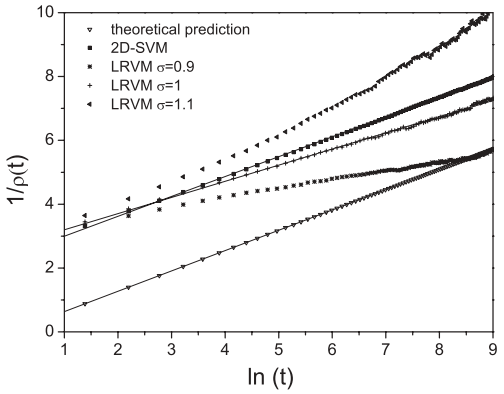

FIG. 4. Plot of $\frac{1}{\rho}$ versus $\ln(t)$ for $\sigma = 1$, 1.1, and 0.9. Numerical results and theoretical predictions of the 2D SVM are also included. Solid lines correspond to the fit with Eq. (2). More details in the text.

of σ close to $\sigma = 1$. This fact adds evidence to the assumption, which is further discussed later, that $\sigma = 1$ is a critical or a transition point where the LRVM behaves as the SVM at the critical dimension ($d_c = 2$). Furthermore, the maximum shown in the inset in Fig. 2(b) can be used to identify different regimes of the dynamic behavior of the LRVM; indeed on the right-hand side of the maximum the model exhibits an ordering dynamics, while on the left-hand side, only steady states are found.

All these behaviors have been verified by extending the measurement time by decades until $t = 3 \times 10^5$ MCS (see Fig. 3), focusing the simulations on some representative values of the control parameter, namely, $\sigma = 1.1$, 1.5, 2.0, and 5.0. Also, suitable system sizes are selected to make sure that finite-size effects do not affect the dynamic behavior, in agreement with the finite-size studies discussed in Sec. III B.

For $0.7 < \sigma \leqslant 1$ [see Fig. 1(a)] a crossover zone between the already described extreme regimes is observed. Here, it is no longer possible to estimate a steady-state value from the exponential decay, but a power-law decay is observed with an exponent close to 0. For $\sigma = 1$, the interface density decay can be fitted according to a logarithmic dependence on the time, given by

$$\rho(t) = \frac{A}{\ln(t)}. \qquad (2)$$

Figure 4 shows that $1/\rho$ follows a linear dependence on $\ln(t)$, with a slope $1/A = 0.52(1)$, which strongly suggests the particular nature of the data corresponding to $\sigma = 1$. Departures from this behavior are clearly observed for $\sigma = 0.9$ and $\sigma = 1.1$. This logarithmic dependence was predicted for the 2D SVM based on a correspondence with a system of coalescing random walks [8]. In that case, the constant $A = 2\pi D$, where $D = 1/4$ is the diffusion constant of the underlying random walk, was calculated [8]. The excellent agreement between our simulation results and the analytic prediction for the 2D SVM is also shown in Fig. 4. Furthermore, other models belonging to the 2D SVM universality class also present the same logarithmic dependence, but with different effective diffusion constants [8]. The before described picture further supports the conjecture about the 2D SVM-like behavior of the proposed LRVM for $\sigma = 1$, with an effective diffusion constant $D = 0.306(6)$. The larger value of the effective diffusion constant could be related to the long-range interactions present in our model.

To gain insight into the coarsening process, the cluster-size distributions for systems of size $L = 10^6$ are studied for different σ values and different times, as shown in Fig. 5(a). Furthermore, both the 1D SVM and the 2D SVM are also simulated for the sake of comparison. Three behaviors are demonstrated in Fig. 5(a), in agreement with the dynamic results. To study these behaviors, representative σ values have been selected. For $\sigma = 0.2$ a stationary narrow distribution is observed for $t \leqslant 3000$ [see Fig. 5(b)], in agreement with the slow decay of $\rho(t)$ shown in Fig. 1(a) for early times. The maximum value of the cluster-size distribution function is found to be close to 1, indicating the presence of rather small clusters (e.g., monomers, dimers, etc.). This result is consistent with the dynamic behavior suggested by the snapshot collection corresponding to $L = 10^4$, shown in Fig. 6(a), where the horizontal axes correspond to time evolution, and black and white squares represent states $s_i = 1$ and $s_i = -1$, respectively. In Fig. 6(a) a smooth granulated or uniform texture can be observed before the finite-size effect becomes relevant, that is, for $t < 1000$ MCS and for this system size. Subsequently, and for this sample, a fast decay into the absorbing state with all spins corresponding to $s_i = 1$ is observed, as expected for finite-size systems. The other extreme behavior corresponds to $\sigma \geqslant 5$ [see Fig. 5(d)], where the cluster-size distribution presents a maximum for larger cluster sizes. For $\sigma = 5$ a sharp maximal value close to 1 and other time-dependent maxima that shift to larger sizes with time are observed [see Fig. 5(d)]. This result is consistent with a coarsening process as suggested by Fig. 6(d), where a collection of snapshots corresponding to a sample of size $L = 10^4$ indicates the fast increase in cluster size. As shown in Fig. 5(d), the larger-size maximum overlaps with the distribution measured for the 1D SVM. Furthermore, cluster-size distributions corresponding to $\sigma = 10$ are coincident with the 1D SVM distribution. In an intermediate zone, Fig. 5(c) shows that for $\sigma = 1.0$ the cluster-size distribution follows

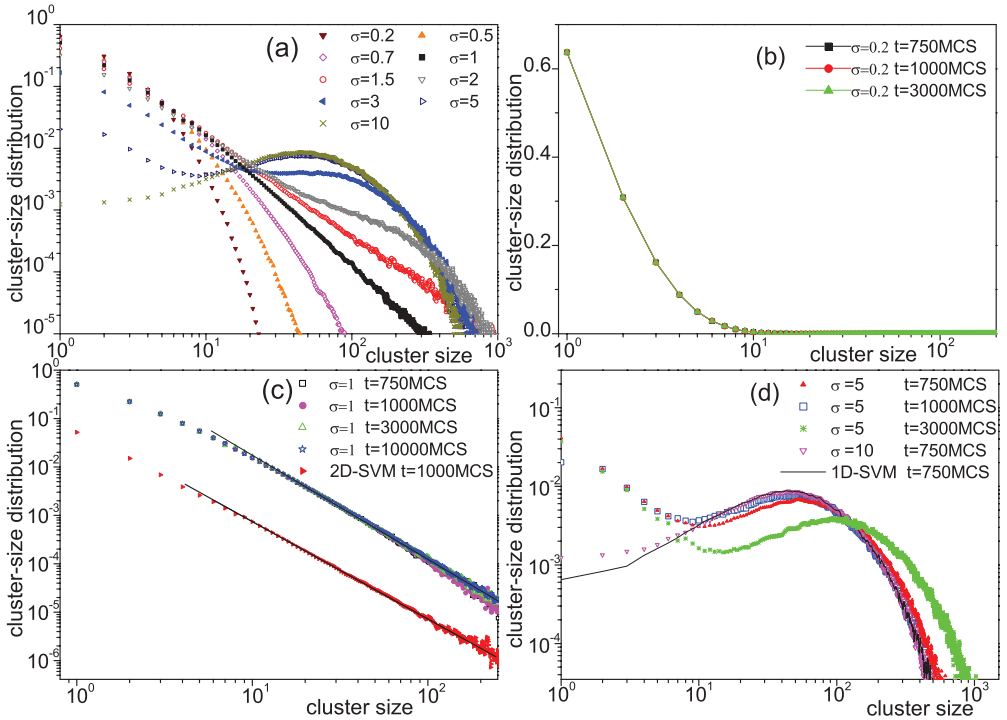

FIG. 5. (Color online) Cluster-size distributions corresponding to samples of size L^6 and different times. (a) For different values of the σ parameter and $t = 750$ MCS. (b) For $\sigma = 0.2$. (c) For $\sigma = 1$; the distribution for 2D SVM is also included and the solid lines correspond to power-law fits. (d) For $\sigma = 5$ and $\sigma = 10$; the distribution for 1D SVM is also included. More details in the text.

a power-law decay, independently of time, with an exponent given by $\mu = 2.09(6)$. This exponent is very close to the result corresponding to the 2D SVM, $\mu = 2.02(3)$, which has also been measured for the sake of comparison. The power-law behavior is compatible with a critical cluster-size distribution where clusters of all sizes are present. This scenario is also suggested by the snapshot collection corresponding to $L = 10^4$ [see Fig. 6(b)]. Furthermore, Fig. 6(b) shows a slow coarsening process compatible with a logarithmic dynamics of the interface density. A similar power-law behavior of the cluster-size distribution is obtained for $\sigma = 1.5$ [see Fig. 5(a)] but with a smaller exponent [$\mu = 1.62(1)$], in agreement with the occurrence of a faster dynamics. The latter observation can be understood as a crossover behavior shown for values of $\sigma \gtrsim 1$. The smaller exponent μ indicates the existence of domains of larger sizes, as can be inferred from Fig. 6(c), where a snapshot collection corresponding to $L = 10^4$ is presented.

B. Study of finite-size effects

The presence of finite-size effects on the ordering dynamics for the different regimes is shown in Figs. 7 and 8, for $\sigma < 1$ and $\sigma \geqslant 1$, respectively. Focusing our attention on the case $\sigma = 0.2$ [see Fig. 7(a)], which belongs to the regime where states decaying exponentially are observed, the lifetime τ increases with the system size. In these cases the time evolution of the density of interfaces is given by

$$\rho(t) = \rho_0 e^{-t/\tau}, \tag{3}$$

and by fitting the measured time evolution with the aid of Eq. (3), one can determine both the lifetime (τ) of the interfaces and the steady-state value ρ_0 corresponding to the thermodynamic limit. The latter value gives an estimate of the average size of the domains since one expects that $l = \rho_0^{-1}$.

The corresponding fits are shown by solid lines in Fig. 7(a) and the resulting parameters are listed in Table I. From these results a power-law dependence of the form $\tau \propto L^{\omega}$, with $\omega = 0.99(1)$, is obtained (see Fig. 9), in agreement with the behavior of the SVM corresponding to a regular network in $d = 3$ and complex networks such as random networks [6], small-world networks [5], and random graphs [16]. In the case of Barabási Albert network [7] this scaling is obtained in the case of a link-update dynamics.

A similar analysis applied to data obtained for $\sigma = 0.8$ and 0.9 yields $\omega = 1.01(1)$ and 0.99(1), respectively.

TABLE I. Estimated values of the average interface density (ρ_0) of the steady state and the lifetime (τ) of the interfaces, obtained by fitting the data with the aid of Eq. (3). Results corresponding to $\sigma = 0.2$ and systems of different sizes (L). The number of different realizations (n_s) is also indicated for each L.

L	ρ_0	τ (MCS)	n_s
5×10^3	0.444(1)	$3.45(8) \times 10^3$	3×10^3
1×10^4	0.448(1)	$6.85(2) \times 10^3$	2.5×10^3
2×10^4	0.449(1)	$1.29(2) \times 10^4$	2×10^3
5×10^4	0.449(1)	$3.13(3) \times 10^4$	5×10^2
1×10^5	0.450(1)	$6.29(4) \times 10^4$	5×10^2

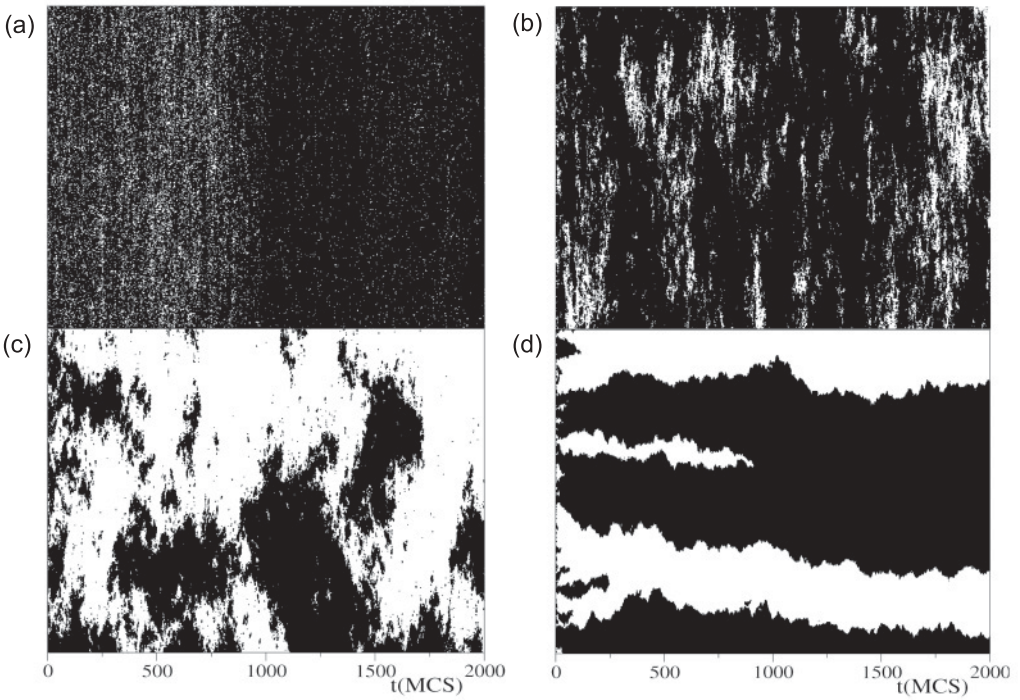

FIG. 6. A collection of snapshots of part of a chain of $L = 10^4$ spins (vertical axis), where black points represent sites in state $s_i = 1$, while sites in state $s_i = -1$ are white. The horizontal axis corresponds to the time evolution of 1D configurations. (a) For $\sigma = 0.2$ a slow regime is clearly observed at $250 \leqslant t \leqslant 750$ MCS, which is followed by a fast decay to the absorbing state with all sites in state $s_i = 1$. (b) For $\sigma = 1$ a slow coarsening process characterized by domain sizes in all scales is observed. (c) For $\sigma = 1.5$ an ordering process, such as a coarsening of grains or a gross texture, can be observed. (d) For $\sigma = 5$ the time evolution of the snapshots shows a fast ordering process of compact domains. More details in the text.

Based on the results already discussed, and aiming to provide a unified description of the decay process, we propose the following dynamic scaling relationship:

$$\rho(t,L) \propto \frac{L}{\tau} f(t/\tau), \tag{4}$$

where $f(t/\tau)$ is a suitable scaling function. Figure 10(a) shows the collapse of the data shown in Fig. 7(a), obtained by taking a lifetime scaling given by $\tau \propto L^1$, in agreement with previous results obtained for this regime, that is, $\omega \simeq 1$ (see also Fig. 9 and Ref. [6]). In this way, one has a scaling function of the form $f(r/\tau) \sim e^{-t/\tau}$.

So, the proposed scaling relationship allows us to determine the lifetime τ for any regime. In this way, for the $\sigma = 1$ regime, the collapse of the data shown in Fig. 8(a) is obtained by taking $\tau \propto L\ln(L)$ [see Fig. 10(b)]. It is worth mentioning that this result is the same as that reported for the SVM with $d_c = 2$.

In contrast, for the power-law regime, the result obtained for $\sigma = 1.5$ leads to $\tau \propto L^{1.4}$ [see Figs. 8(b) and 10(c)]. As shown in Fig. 10(d), with increases in σ this behavior approaches

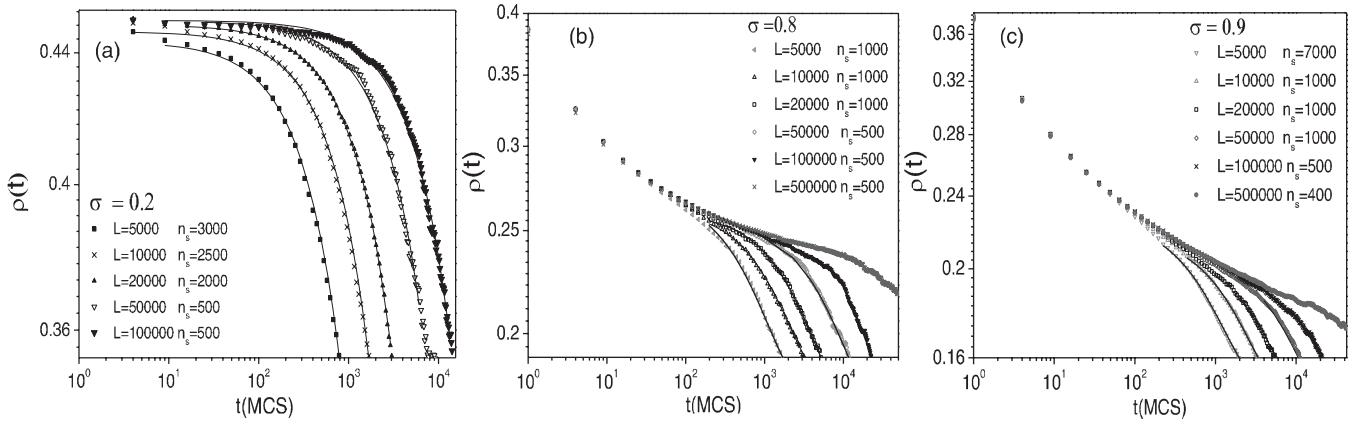

FIG. 7. Log-log plots of the time evolution of the average interface density $\rho(t)$ for systems of different sizes (L): (a) $\sigma = 0.2$, (b) $\sigma = 0.8$, and (c) $\sigma = 0.9$. System sizes and number of averaged samples (n_s) are also indicated, while solid lines correspond to the fit of data with the aid of Eq. (3). More details in the text.

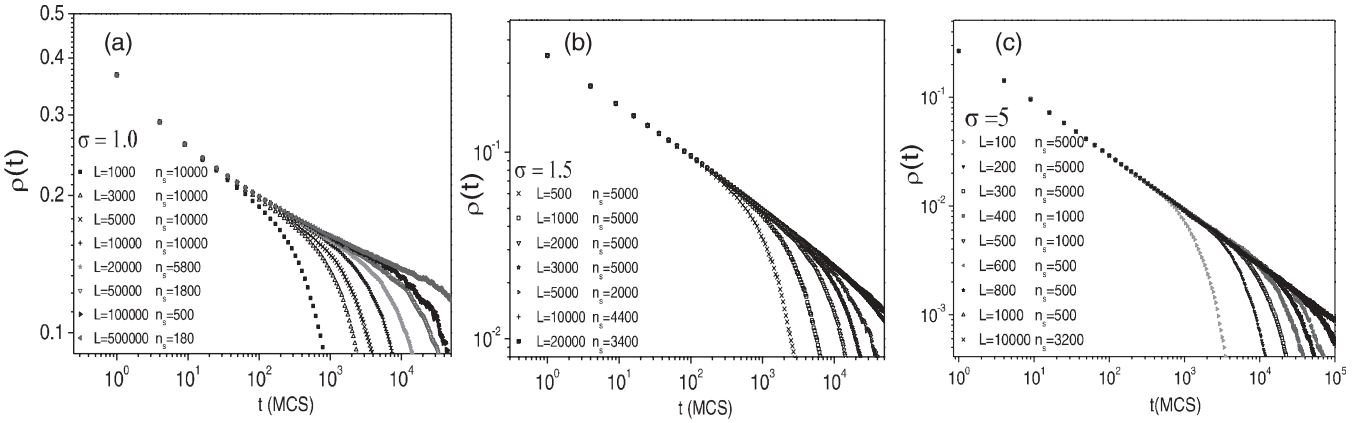

FIG. 8. Log-log plots of the time evolution of the average interface density $\rho(t)$ for systems of different sizes (L): (a) $\sigma = 1$, (b) $\sigma = 1.5$, and (c) $\sigma = 5$. System sizes and number of averaged samples (n_s) are also indicated. More details in the text.

that corresponding to 1D SVM given by $\tau \propto L^2$, which is already reached for $\sigma = 5$. This scaling behavior of τ was also obtained for a structured scale-free network [6], which has an effective dimension $d_{\text{eff}} = 1$.

To further clarify and support our simulation results, we also calculate the first ($n = 1$) and second ($n = 2$) moments of the long-range interaction distance distribution given by

$$\langle r^{(n)} \rangle_\sigma = \int_1^L r^{(n)} \frac{A_\sigma}{r^{d+\sigma}} dr, \tag{5}$$

where

$$A_\sigma = \frac{1}{\int_1^L 1/r^{1+\sigma} dr}. \tag{6}$$

Furthermore, we also evaluate the fluctuations of the mean distance according to

$$\langle \Delta r \rangle = \sqrt{\langle r^{(2)} \rangle - \langle r \rangle^2}. \tag{7}$$

The main idea is to establish a relationship among the different behaviors observed for different σ regimes, their effective dimensionality, and the way these magnitudes scales in the $L \to \infty$ limit. The results obtained are reported in Table II. For $\sigma < 1$, $\langle r \rangle$, and $\langle r^{(2)} \rangle$ exhibit strong size dependence. Furthermore, both are divergent values in the thermodynamic limit. These results correspond to a high-connectivity regime, characteristic of higher dimensions. For $\sigma = 1$ a much slower logarithmic divergence is found for the first moment ($\langle r \rangle$), whereas for $\langle r^{(2)} \rangle$ a linear dependence on the size is found. It is worth mentioning that although both moments here are already divergent in the thermodynamic limit, the size dependence of the mean value is much weaker than the fluctuations at a fixed

TABLE II. Analytical results for the first ($\langle r \rangle$) and second ($\langle r^{(2)} \rangle$) of the long-range interaction distance distribution, obtained with the aid of Eq. (5) and corresponding to different values of the control parameter σ.

σ regimen	Size dependence of moments	Asymptotic behavior with size (L)	Behavior $L \to \infty$
$\sigma = 0$	$\langle r \rangle = \frac{(L-1)}{\ln(L)}$	$\langle r \rangle \sim \frac{L}{\ln(L)}$	∞
	$\langle r^{(2)} \rangle = \frac{(L^2-1)}{2\ln(L)}$	$\langle r^{(2)} \rangle \sim \frac{L^2}{2\ln(L)}$	∞
$0 < \sigma < 1$	$\langle r \rangle = \left(\frac{\sigma}{1-\sigma}\right) \frac{(L^{1-\sigma}-1)}{(1-L^{-\sigma})}$	$\langle r \rangle \sim \left(\frac{\sigma}{1-\sigma}\right) L^{1-\sigma}$	∞
	$\langle r^{(2)} \rangle = \left(\frac{\sigma}{2-\sigma}\right) \frac{(L^{2-\sigma}-1)}{(1-L^{-\sigma})}$	$\langle r^{(2)} \rangle \sim \left(\frac{\sigma}{2-\sigma}\right) L^{2-\sigma}$	∞
$\sigma = 1$	$\langle r \rangle = \frac{\ln(L)}{(1-L^{-1})}$	$\langle r \rangle \sim \ln(L)$	∞
	$\langle r^{(2)} \rangle = \frac{(L-1)}{(1-L^{-1})}$	$\langle r^{(2)} \rangle \sim L$	∞
$1 < \sigma < 2$	$\langle r \rangle = \left(\frac{\sigma}{\sigma-1}\right) \frac{(1-L^{1-\sigma})}{(1-L^{-\sigma})}$	$\langle r \rangle \sim \left(\frac{\sigma}{\sigma-1}\right) (1 - L^{1-\sigma})$	$\frac{\sigma}{\sigma-1}$
	$\langle r^{(2)} \rangle = \left(\frac{\sigma}{\sigma-2}\right) \frac{(1-L^{2-\sigma})}{(1-L^{-\sigma})}$	$\langle r^{(2)} \rangle \sim \left(\frac{\sigma}{\sigma-2}\right) (1 - L^{2-\sigma})$	∞
$\sigma = 2$	$\langle r \rangle 2 \times \frac{(1-L^{-1})}{(1-L^{-2})}$	$\langle r \rangle \sim 2 \times (1 - L^{-1})$	2
	$\langle r^{(2)} \rangle = \frac{2\ln(L)}{(1-L^{-2})}$	$\langle r^{(2)} \rangle \sim 2 \times \ln(L)$	∞
$\sigma > 2$	$\langle r \rangle = \left(\frac{\sigma}{\sigma-1}\right) \frac{(1-L^{1-\sigma})}{(1-L^{-\sigma})}$	$\langle r \rangle \sim \left(\frac{\sigma}{\sigma-1}\right) (1 - L^{1-\sigma})$	$\frac{\sigma}{\sigma-1}$
	$\langle r^{(2)} \rangle = \left(\frac{\sigma}{\sigma-2}\right) \frac{(1-L^{2-\sigma})}{(1-L^{-\sigma})}$	$\langle r^{(2)} \rangle \sim \left(\frac{\sigma}{\sigma-2}\right) (1 - L^{2-\sigma})$	$\frac{\sigma}{\sigma-2}$
$\sigma \to \infty$	$\langle r \rangle \sim 1 \times \frac{(1-L^{1-\sigma})}{(1-L^{-\sigma})}$	$\langle r \rangle \sim 1 - L^{1-\sigma}$	1
	$\langle r^{(2)} \rangle \sim 1 \times \frac{(1-L^{2-\sigma})}{(1-L^{-\sigma})}$	$\langle r^{(2)} \rangle \sim 1 - L^{2-\sigma}$	1

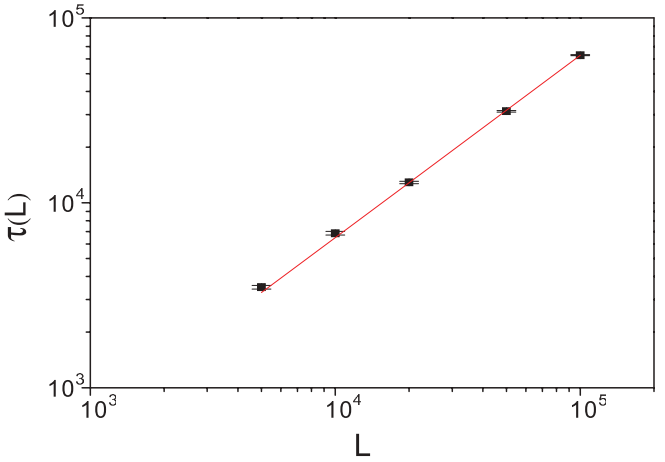

FIG. 9. (Color online) Log-log plot of the lifetime of the average interface density $\rho(t)$ versus the system size L, as obtained for $\sigma = 0.2$. Solid line indicates the power-law fit. More details in the text.

length (i.e., for $L = 10^6$, one has $\langle r \rangle \sim 13$, and $\langle \Delta r \rangle \sim 1000$). Furthermore, this logarithmic dependence can be understood as a limit point between a mean-field behavior, where the number of neighbors has a linear dependence on the size and any subcritic dimension of the SVM where the number of neighbors is independent of the size. This particular situation, with the addition of the slow logarithmic dynamics also measured, is suggested as a plausible cause for the observation of a critical-type behavior. The region $1 < \sigma < 2$ can be understood as another crossover behavior where $\langle r \rangle$ is here a σ-dependent convergent magnitude, but the fluctuations are still large, in a way similar to the $\sigma = 1$ case, but now with a measured power-law coarsening dynamics. For $\sigma > 2$, both moments became convergent, corresponding to an intermediate coarsening regime; furthermore, they depend on σ and, at last, assume (for $\sigma \to \infty$) the expected values of the 1D SVM.

The results already discussed allow us to establish an analogy between the studied LRVM in the $d = 1$ dimension and the SVM in regular and complex networks, providing evidence of an effective multidimensional crossover behavior that is obtained by tuning the control parameter of the strength of the long-range interactions σ: (i) The results obtained for $\sigma \ll 1$ can be related to the dynamic behavior of the SVM observed above the critical dimension, that is, for $d > d_c = 2$, where the system reaches a steady state and the average interface density remains constant. This behavior will remain forever in the thermodynamic limit, but due to the finite size of the samples used in our simulations, a fluctuation will always ultimately drive the system toward one of the two symmetric absorbing states. (ii) For $\sigma = 1$ our results are in agreement with the critical ordering observed at the critical dimension ($d_c = 2$) of the SVM. It is also observed that around this value an intermediate crossover regime is present. In fact, for $0.7 < \sigma \lesssim 1$ a slow dynamic without a scale-free cluster-size distribution is found, while for $1 \lesssim \sigma \leqslant 2$ one has the scale-free cluster-size distribution accompanied by a faster dynamic with well-defined power-law decays. (iii) For $\sigma > 2$ the fluctuations of the mean distance tend to vanish and one observes intermediate (σ-dependent) power-law decays of the interface density with the addition of a well-established coarsening process. (iv) Finally, for $\sigma > 5$, the results obtained are fully consistent with a 1D SVM behavior.

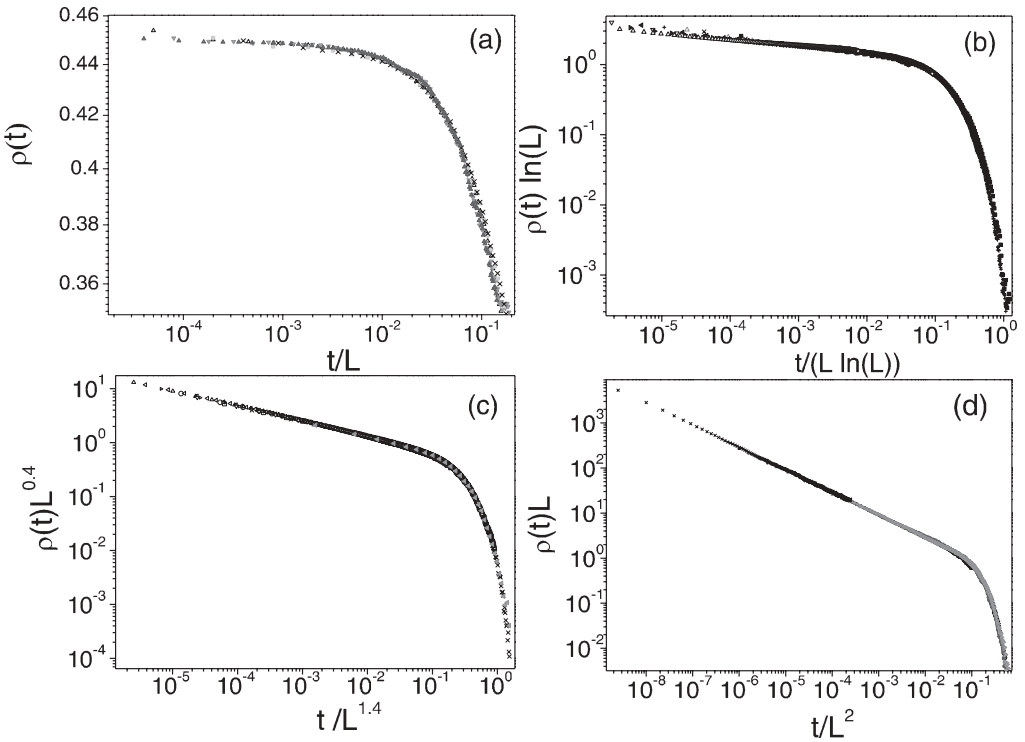

FIG. 10. Scaling plots of the average interface density $\rho(t)$ obtained for systems of different sizes (L) considered in Figs. 7 and 8: (a) $\sigma = 0.2$, (b) $\sigma = 1$, (c) $\sigma = 1.5$, and (d) $\sigma = 5$. More details in the text.

IV. CONCLUSIONS

In the present work an LRVM with probabilistic interactions between spins placed at a distance r given by a distribution $P(r) \propto r^{-(d+\sigma)}$, where σ is a control parameter, is proposed and studied by means of Monte Carlo simulations. The results are analyzed with the aid of dynamic and finite-size scaling arguments. In this way, an interesting dynamic behavior that can be rationalized in terms of an effective multidimensional behavior is obtained by sweeping the control parameter σ. Furthermore, from the scaling analysis of the finite-size effects and the study of the cluster-size distribution, we establish an analogy between the well-known behavior of the SVM—on regular lattices in any dimension and, also, with different types of complex networks—and the value of σ.

In fact, for $\sigma < 1$ the observed nonordering dynamics with a noncoarsening process corresponds to $d > d_c = 2$. For $\sigma = 1$ one has a critical ordering process, which shows up as a logarithmic dynamics, a scale-free cluster-size distribution, and a proper finite-size scaling as in $d_c = 2$. Finally, for $\sigma > 1$ the vanishing of the fluctuations of the long-range mean distance establishes the beginning of a coarsening behavior with a σ-dependent power-law decay of the interface density that, for $\sigma \geqslant 5$, allows one to fully recover the $d = 1$ behavior.

Summing up, the proposed voter model with long-range probabilistic interactions exhibits an effective multidimensional behavior just by tuning the algebraic decay, in a way that σ assumes the role of a switching dimensional control parameter. Furthermore, the study of the proposed long-range voter model in $d = 1$ allows us to gain insight, in a unified fashion, into the behavior of the SVM in any dimension, including the behavior of some complex networks, a subject that poses new and interesting theoretical challenges.

ACKNOWLEDGMENTS

This work was supported by CONICET, UNLP, and ANPCyT (Argentina).

[1] L. Frachebourg and P. L. Krapivsky, Phys. Rev. E **53**, R3009 (1996).
[2] R. Holley and T. M. Ligget, Ann. Prob. **3**, 643 (1975).
[3] F. Vazquez and V. Eguíluz, New J. Phys. **10**, 063011 (2008).
[4] H. Hinrichsen, Adv. Phys. **49**, 815 (2000).
[5] C. Castellano, D. Vilone, and A. Vespignani, Europhys. Lett. **63**, 153 (2003).
[6] K. Suchecki, V. M. Eguíluz, and M. San Miguel, Phys. Rev. E **72**, 036132 (2005).
[7] C. Castellano, V. Loreto, A. Barrat, F. Cecconi, and D. Parisi, Phys. Rev. E **71**, 066107 (2005).
[8] I. Dornic, H. Chaté, J. Chave, and H. Hinrichsen, Phys. Rev. Lett. **87**, 045701 (2001).
[9] P. L. Krapivsky, Phys. Rev. A **45**, 1067 (1992).
[10] K. Suchecki and J. A. Holyst, Physica A **362**, 338 (2006).
[11] M. A. Novak, *Evolutionary Dynamics* (Berkmap, Cambridge, 2006).
[12] F. Vázquez and C. López, Phys. Rev. E **78**, 061127 (2008).
[13] R. Lambiotte and S. Redner, J. Stat. Mech. Theory Exp. (2007) L10001.
[14] C. Castellano, M. A. Muñoz, and R. Pastor-Satorras, Phys. Rev. E **80**, 041129 (2009).
[15] D. Vilone and C. Castellano, Phys. Rev. E **69**, 016109 (2004).
[16] V. Sood and V. Redner, Phys. Rev. Lett. **94**, 178701 (2005).
[17] M. A. Bab, G. Fabricius, and E. V. Albano, Europhys. Lett. **81**, 10003 (2008).
[18] M. A. Bab and E. V. Albano, Eur. Phys. J. B **63**, 521 (2008).